JOURNAL OF MATERIALS SCIENCE: MATERIALS IN MEDICINE **16** (2005) 1221 – 1229

Physical and biological characterizations of a novel multiphase anodic spark deposition coating to enhance implant osseointegration

CARMEN GIORDANO[1,*], ROBERTO CHIESA[1], ENRICO SANDRINI[1], ALBERTO CIGADA[1], GIANLUCA GIAVARESI[2], MILENA FINI[2], ROBERTO GIARDINO[2]
[1]*Department of Chemistry, Materials and Chemical Engineering "G.Natta", Polytechnic of Milan, Via Mancinelli, 7, Milan, Italy*
E-mail: carmen.giordano@polimi.it
[2]*Department of Experimental Surgery, Rizzoli Orthopaedic Institute, Bologna, Italy*

The present study assessed *in vitro* the short-term cellular response to surface physico-chemical properties of a new, purposed bioactive surface treatment called BioSpark™ performed on simply machined and on sand-blasted titanium. Material characterisation was carried out using scanning electron microscopy, energy dispersion spectroscopy, laser profilometry, and thin film X-ray diffraction. The *in vitro* biological study showed a suitable cellular response with adhesion and spreading level comparable for all the tested specimens. The proliferation analysis demonstrated that all the surfaces successfully supported cellular colonisation; in particular, higher cellular proliferation activity was observed on the BioSpark™-treated materials, with values higher than machined titanium. The results suggest that the BioSpark™ treatment represents a smart way to enhance osteoblastic cellular colonisation and thus improve osteointegration processes of machined and sandblasted titanium for orthopaedic and dental implants.

1. Introduction

Progress in recent years in the modification of surfaces by chemical, electrochemical, photochemical and plasma-chemical techniques has opened new possibilities to tailor the surface properties of widely exploited implantology materials such as titanium (Ti) and Ti alloys. A great deal of current research focuses on the effect of different chemical and electrochemical treatments on the bioactivity of such materials [1–4].

The aim of these treatments is to modify Ti in order to achieve surface titanium oxide (TiO_2) by mimicking hydroxyapatite mineralization and osteoconductive properties.

A new double-plasma electrolysis oxidation process (PEO), called BioSpark™, was recently developed [5], and applied to Ti and its alloys. BioSpark™-treated surfaces exhibited highly micro-porous and nano-roughened textured TiO_2, whose main phase was reported to be anatase [6]. Furthermore, it was also reported that this new surface spontaneously promotes calcium-phosphate cluster nucleation from simulated body fluids (SBF) even after short-time SBF soaking [6, 7]. Indeed, short-term cellular response studies demonstrated that BioSpark™-treated surfaces supported well MG63 osteoblastic-like cell adhesion and proliferation when compared with smooth, sandblasted or acid-etched Ti surfaces [1, 7]. MG63 human osteosarcoma cells are known to be advantageous for studies of bone cell metabolism because they show several characteristics of immature osteoblasts and can be used as a model to investigate the early stages of osteoblastic response [8].

The aim of the present work was to assess *in vitro* bone cellular response to physicochemical and topographical properties of simply machined and sandblasted Ti textures before and after surface treatment with the new purposed bioactive method called BioSpark™. Surface features were previously investigated to: (a) analyse surface morphology (scanning electron microscopy, SEM); (b) assess the procedure influence on surface chemical composition (energy dispersion spectroscopy, EDS); (c) assess the presence of crystalline TiO_2 and its structure on material surface (thin film X-ray diffractometry, TF-XRD). Then, MG63 osteoblastic-like cell morphology and adhesion were evaluated on sample surfaces at 6 and 24 h after cell seeding, as well as MG63 cell proliferation at specific time points (1, 3, 7 days of cell culturing) by using the Alamar Blue™ assay [9].

*Author to whom all correspondence should be addressed.

2. Materials and methods

2.1. Sample preparation

All Ti samples used in this work were obtained from a sheet of commercially-pure grade-2 Ti (Toresin Titanio, Padova). Coupons ($\varnothing 10 \times 1$ mm^3) were cut with a mechanical cutter available at Tempe (CNR Milan) and rinsed by ultrasonic rinsing (Branson Automatic Cleaner, UK) in acetone (RPE Carlo Erba or Sigma Aldrich, Italy) for 5 min and in distilled water for the same time to degrease and to clean the surface from contaminants. Four different surface finishing were prepared:

- SM-TI: machined smooth Ti without any further treatment.
- SB-TI: rough Ti achieved by sandblasting.
- SM-BSP: BioSpark^{TM} electrochemical surface treatment by Anodic Spark Deposition (ASD) and alkali treatment [6, 9] carried out on SM-TI.
- SB-BSP: BioSpark^{TM} electrochemical surface treatment by ASD and alkali treatment [6, 9] carried out on SB-TI.

2.1.1. SB treatment procedure

Ti coupons were sandblasted with Al_2O_3 (particle sizes ranged from 50 to 300 μm), with a pressure flow of 3 kgf/cm^2) and kept at an angle of 90° to the surface. Sandblasting lasted 60 s per sample.

2.1.2. BSP treatment procedure

Ti surface was prepared in an electrochemical cell by a double-step ASD technique [1–3], followed by alkali etching. A variable DC power supply (BVR1200-500-1.5 Belotti Variatori S.r.l., Italy) and two voltmeters were used to supply power to the circuit and to monitor the voltage gap between cathode and anode, as well as between cathode and points of the electrolytic solution in between the two electrodes. The solution underwent continuous magnetic stirring in a double-wall glass beaker. Electrolytic solution temperature was monitored and kept at 0 °C (±2 °C) by the flowing of a refrigerating fluid through the external and the inner wall of the beaker. Specimens were connected one by one to the anode. A Teflon sleeve was used to shield the specimen surfaces and to avoid sparking at the atmosphere-sample-electrolyte solution interface. The cathode was formed by a c.p. Ti grade-2 cylindrical-shaped net, whose surface was about 60 times bigger than the surface of the anodising sample. BSP protocol involves a two-consecutive-step ASD process (label ASD1 and ASD2) carried out in different electrolytes at different voltage ranges, and a further hot alkali etching process through the final BSP surface is achieved [6]. Full details of the BSP surface modification technique and sample preparation techniques have been reported elsewhere [4].

2.2. Physicochemical property analysis

All the tests were performed at least in triplicate on five specimens for each sample. The morphology of the different surfaces was analysed by means of SEM (STEREOSCAN 430—Leica Cambridge Instruments, Great Britain) uploaded with backscattered electrons detector. All samples investigated with SEM were sputter-coated with gold (Sputter Coater SC7640, Polaron).

Non-sputter-coated surfaces, except for SM-BSP, were investigated also by EDS (Link eXL analyser, with Si(Li) detector PENTAFET PLUS, Great Britain) and the software package ZAF-4/FLS for massive sample analysis. EDS allowed qualitative understanding of the influence of different procedures on the chemical composition of the exposed surface and, evaluation of the presence of machining contaminants after washing and degreasing.

TF-XRD was carried out to achieve better knowledge of the crystalline structure of the differently treated surfaces and, to assess the presence of crystalline TiO_2 and other oxides as a result of oxidation processes on the Ti surface and sandblasting procedure respectively. Samples surface properties were investigated with thin-film X-ray diffraction (Siemens D500 Kristalloflex, Germany) at 40 mA and 40 kV, before SBF soaking and after soaking.

The roughness parameters were calculated on 5.6 mm-long profiles, and every measurement was repeated 5 times. Measurements were acquired using a (LPM) 3D laser profilometer (UBM-Microfocus Compact, NanoFocus AG, Germany).

2.3. *In vitro* biological response

The samples were tested after sterilisation by ethanol absolute followed by UV irradiation (254 nm). Tissue culture plate polystyrene (Corning- Costar Celbio, Italy) was used as negative control for cellular elution and cellular metabolic activity studies. The human osteosarcoma cell line MG63 (ECACC) was cultured as previously described [9]. After trypsinisation, cell viability was assessed using the Trypan Blue exclusion dye (Sigma-Aldrich). The specimens were placed in 24-well tissue culture plates and MG63 seeded (50 μl of 2×10^5 cells/ml suspension); cells were allowed to adhere in the incubator for 1 h. Finally, the samples were flooded with 1 ml of culture medium and incubated at 37 °C.

2.3.1. Cellular adhesion and morphology

At selected time points (6 and 24 h), the samples (2 replicates) were used for cell adhesion and morphology evaluations by means of SEM. MG63 were fixed with 1.5% w/w glutaraldehyde (Fluka) in 0.1 M sodium cacodylate (Fluka) at 4 °C, dehydrated through a series of ethyl alcohol (BDH) concentration (from 20 up to 100% v/v in distilled water) followed by a series of hexamethyldisilazane (Sigma-Aldrich) solutions (from 25%, up to 100% v/v in ethyl alcohol) and then air dried. The samples were sputter coated (Edwards, Sputter Coater S150B, 1 minute at 15–20, 10^{-1} mmHg) before examination by SEM (accelerating voltage of 10 keV).

2.3.2. Cell proliferation assay

After cell seeding, at each time point (1, 3, 7 days), culture medium was replaced with 1 ml of 10% v/v Alamar Blue (Serotec) solution in culture medium and the samples (4 replicates) incubated for 4 h. Then, 100 μl (3 replicates) of solution taken from each well was transferred to a 96-well plate and the absorbance measured by a Tecan Genius Plus plate reader (test wavelength: 570 nm; reference wavelength: 630 nm). The samples, rinsed with PBS, were flooded with 1 ml of culture medium and returned back in culture.

2.4. Statistical analysis

Statistical analysis was performed using the SPSS v.12.1 software (SPSS Inc., Chicago, Illinois, USA). Data are reported as mean $\pm$ SD at a significance level of $p < 0.05$. After having verified the normal distribution and the homogeneity of the variance, ANOVA test, followed by Bonferroni t test, were performed to highlight any significant differences between surface treatments in terms of physicochemical properties and cytocompatibility.

3. Results

3.1. Physicochemical property analysis

Machined smooth Ti (SM-TI) presented a regular texture with low linear peaks and smooth edges (Fig. 1(a)). On the contrary, rough, sandblasted Ti (SB-TI) exhibited an irregular morphology with high peaks and wide valleys spread all over the Ti surface, with embedded Al_2O_3 particles protruding from the Ti surface (Fig. 1(b)). SM-BSP texture was more regular than SM-TI and many round crests and deep pores were clearly visible on the surface (Fig. 1(c)). Its whole surface was covered by a thin nanostructured coating similar to the micro porous morphology, not present after the ASD2 process (data not shown), but formed only after alkali treatment [6]. Finally, SB-BSP (Fig. 1(d)) surface exhibited a perfect match with SB-TI texture, with untreated sand grains still appearing on the native surface.

EDS analysis of SM-TI surface showed the presence of Ti and oxygen (Fig. 2(a)), while on SB-TI aluminium and oxygen signals confirmed the presence of remaining sandblasting particles on the native surface (Fig. 2(b)). Calcium, phosphorous and oxygen peeks were found besides the peaks of Ti and oxygen on SM-BSP textures (Fig. 2(c)). Even on SB-BSP the presence of aluminium due to sandblasting treatment was detected within calcium, oxygen and phosphorus surface enrichment after BSP treatment (Fig. 2(d)).

TF-XRD analysis carried out on SM-TI showed that the only crystalline phase detectable was that of Ti (Fig. 3(a)) and on SB-TI it confirmed that the sandblasted surface was homogeneously spoiled by alumina powder (Fig. 3(b)). A thin layer of TiO_2 mainly in the anatase phase covered SM-BSP surface (Fig. 3(c)). TF-XRD analysis carried out on ASD1 and ASD2 samples showed that the second anodization step of BSP treatment was the most effective in achieving crystalline TiO_2 growth. The comparison of ASD2 spectra and

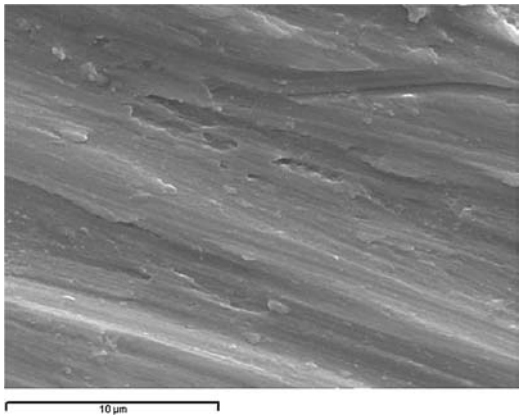

(a)

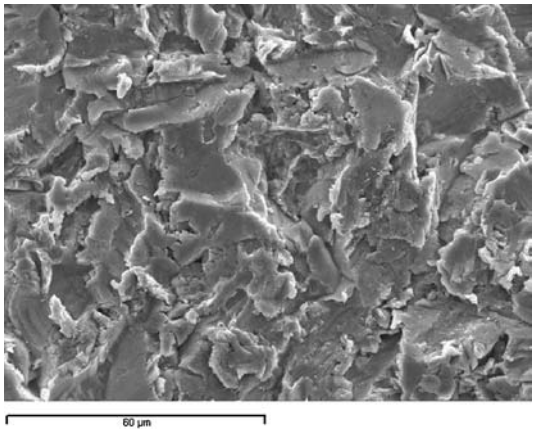

(b)

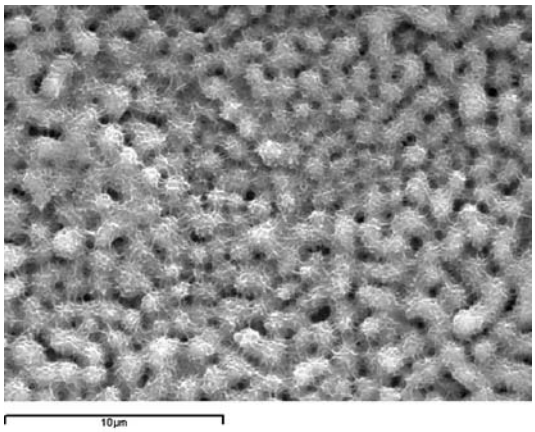

(c)

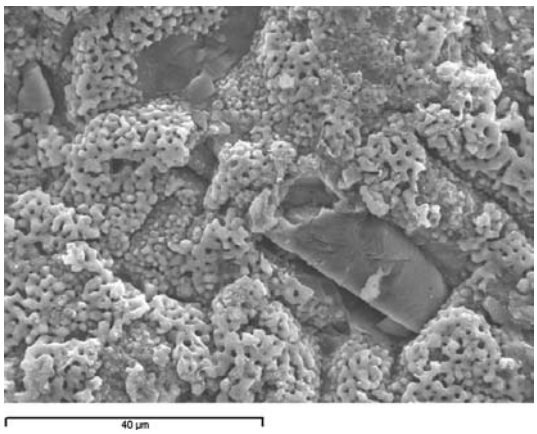

(d)

Figure 1 Scanning electron microscopy of (a) SM-TI: machined Ti; (b): SB-TI: sandblasted Ti; (c): SM-BSP: BioSpark^{TM} treatment on SM-TI; (d) SB-BSP: BioSpark^{TM} treatment on SB-TI.

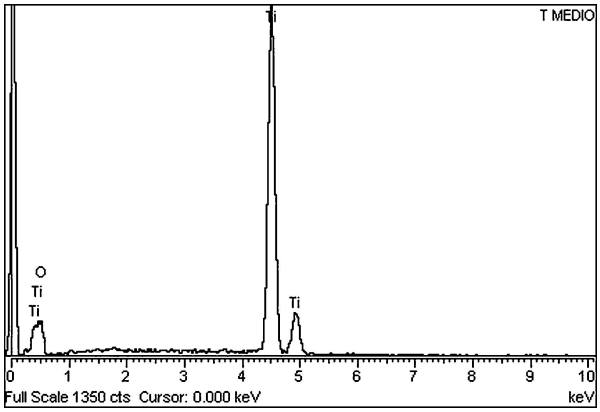

(a)

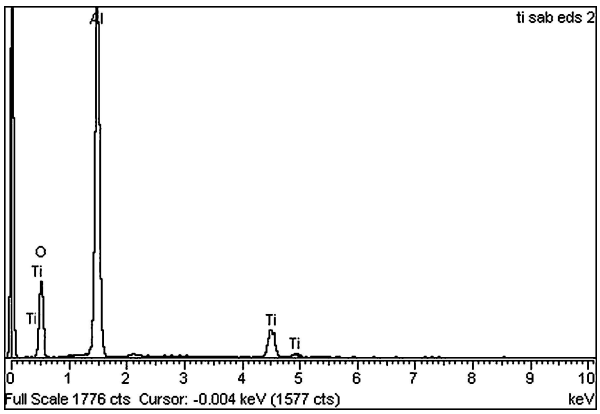

(b)

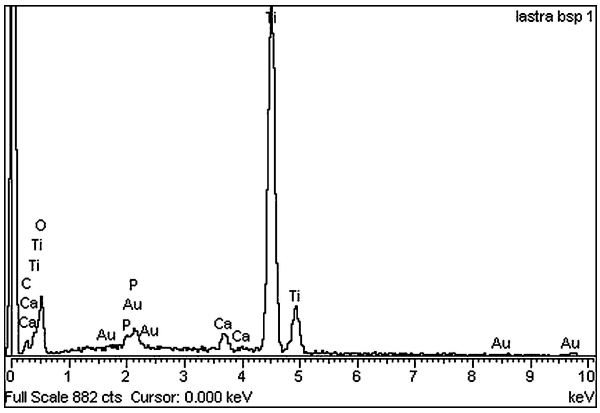

(c)

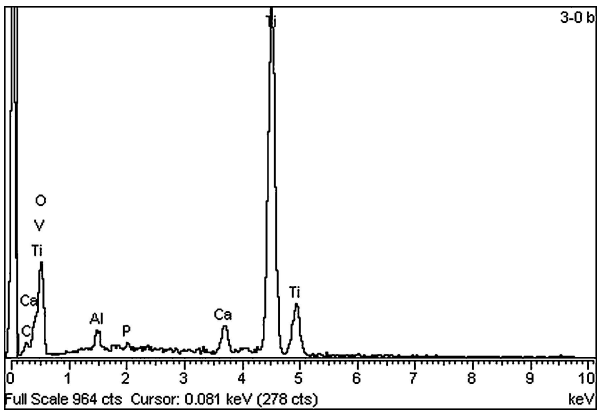

(d)

Figure 2 Energy dispersive spectroscopy of: Scanning electron microscopy of (a) SM-TI: machined Ti; (b): SB-TI: sandblasted Ti; (c): SM-BSP: BioSpark^{TM} treatment on SM-TI; (d) SB-BSP: BioSpark^{TM} treatment on SB-TI.

BSP final spectra showed that alkali treatment slightly modified surface crystalline phases, thus favouring the growth of rutile phase. In the end, SB-BSP X-ray spectra confirmed that BSP procedure developed on Ti surface a thin crystalline oxide, a layer mainly composed of anatase. However, it was found that a slight alumina signal was detectable and spoiled the treated surface (Fig. 3(d)).

Basically, surface roughness analysis confirmed what had already been observed by SEM (Table 1). The sand-blasted surface, SB-TI, exhibited the highest average roughness in terms of R_a and R_{max} values. BSP-treated surfaces (SM-BSP and SB-BSP) showed significantly lower R_a parameters (about 38%, $p < 0.01$) than those of SM-TI and SB-TI, respectively, and Sk was around zero, thus confirming what had been observed by SEM, i.e. that every surface exhibited a certain symmetry in peak and valley distribution, except for SB-BSP.

3.2. *In vitro* biological response

3.2.1. Cellular adhesion and morphology

Six hours after cell seeding (Fig. 4), all the tested surfaces showed adherent cells with healthy morphology surrounded by numerous filopodia. In particular, on SB-TI, SM-BSP and SB-BSP, cell filopodia were preferentially anchored on the peaks protruding from the surface (Fig. 4(b)–(d)). Also, on both the BSP-treated samples (Fig. 4(c) and 4(d)), some cells in a more advanced adhesion state showed a very tight adhesion on sample surface, as suggested by flat and almost transparent edges tightly adhering to the surface. Cells anchored on the surface valley edges covering valley slopes were visible on SB-Ti and SB-BSP textures (Fig. 4(b) and (d)).

After 24 h of cell culturing, an increased number of adherent and spread cells with a more flattened cellular morphology and generally shorter and fewer filopodia were observed on all the tested materials (Fig. 5). However, MG63 cells in a more advanced adhesion state were visible only on SM-Ti and SB-TI specimens, with a cellular monolayer covering regions of the sample surface (Fig. 5(a) and (b)). The results obtained for BSP

TABLE I Non-Contact Laser beam profilometry results; sand-blasted materials show much greater roughness than smooth ones, BioSpark^{TM} treatment further reduces roughness both on SM-TI and SB-TI substrates

	SM-TI	SB-TI	SM-BSP	SB-BSP
Ra (μm)	0.47 ± 0.01	1.91 ± 0.17^{a}	0.29 ± 0.03^{b}	$1.19 \pm 0.14^{a,c}$
Rmax (μm)	3.54 ± 0.10	13.60 ± 1.32^{a}	2.24 ± 0.41^{b}	$10.19 \pm 1.00^{a,c}$
Sk	-0.13 ± 0.18	-0.27 ± 0.17	0.07 ± 0.21	-0.77 ± 0.22^{d}
K	3.06 ± 0.17	3.10 ± 0.67	3.12 ± 0.36	4.42 ± 0.77^{d}

SM-TI: machined Ti; SB-TI: sandblasted Ti; SM-BSP: BioSpark^{TM} treatment on SM-TI; SB-BSP: BioSpark^{TM} treatment on SB-TI. Ra: mean of the departures of the roughness profile from the mean line; Rmax: maximum profile valley depth; K: distribution of the profile height around an ideal average line; Sk: distribution symmetry of the profile height around an ideal average line; Bonferroni multiple comparison test $p < 0.01$: [a], *versus* SM-TI; [b], *versus* SB-TI; [c], *versus* SM-BSP; $p < 0.05$:[d], *versus* SM-TI, SB-TI and SM-BSP.

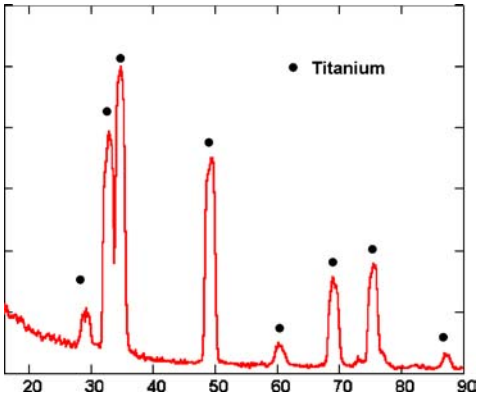

(a)

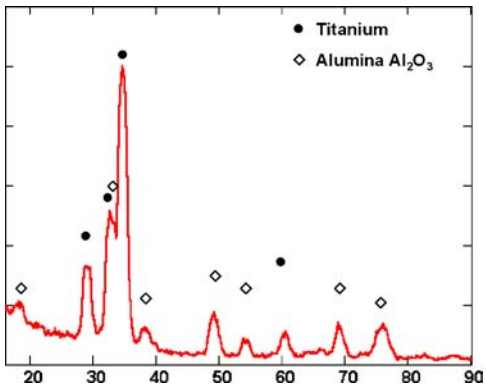

(b)

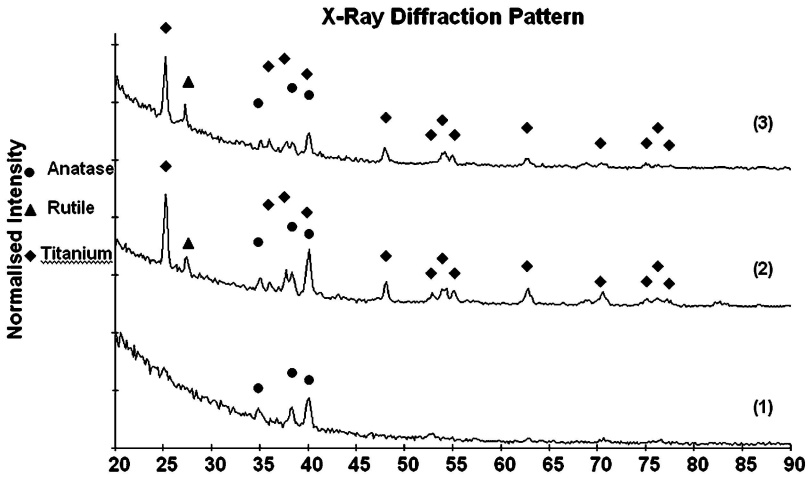

(c)

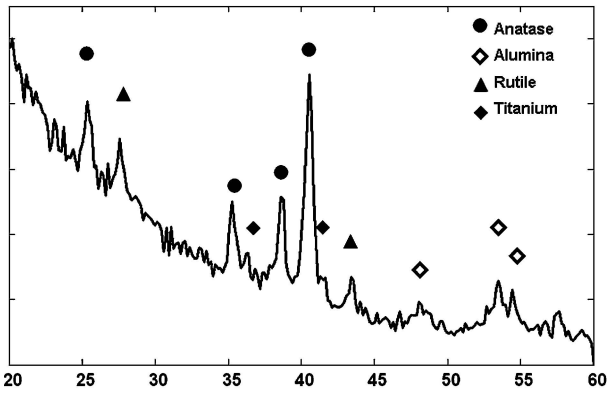

(d)

Figure 3 Thin Film X-ray diffractometry of (a) SM-TI: machined Ti; (b): SB-TI: sandblasted Ti; (c): SM-BSP: BioSpark^{TM} treatment on SM-TI; (d) SB-BSP: BioSpark^{TM} treatment on SB-TI spectra exhibits only Ti peaks, while on SB-TI spectra also alumina peaks can be observed, while on BSP treated substrates high anatase peaks and low rutile peaks appear. In c-1 SM-BSP spectra is shown after first anodisation step; c-2 shows diffraction spectra after the second anodisation, and c-3 shows the final SM-BSP diffraction spectra, exhibiting high anatase peaks as well as Ti, and rutile peaks.

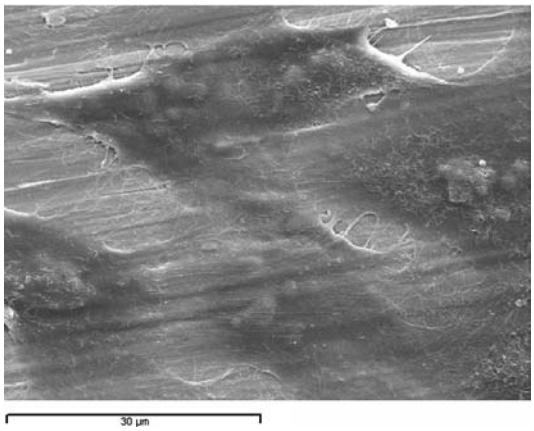

(a)

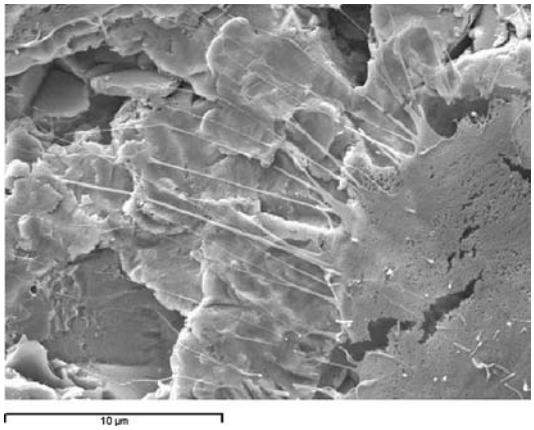

(b)

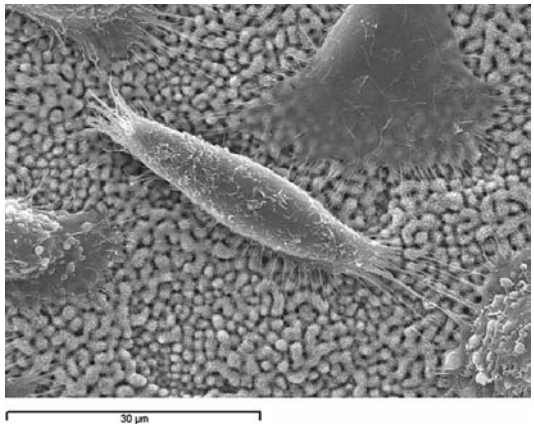

(c)

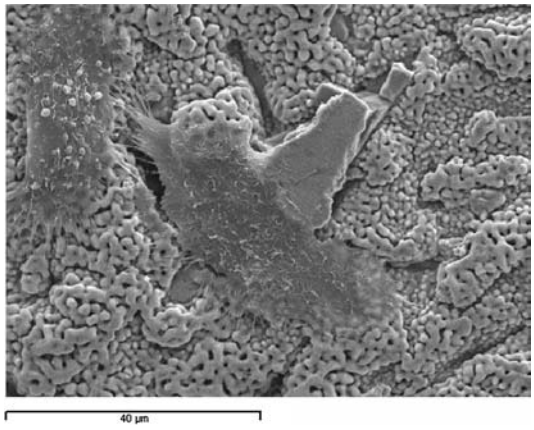

(d)

Figure 4 SEM micrograph of MG63 cells cultured for 6 hours on (a) SM-TI: machined Ti; (b): SB-TI: sandblasted Ti; (c): SM-BSP: BioSpark^{TM} treatment on SM-TI; (d) SB-BSP: BioSpark^{TM} treatment on SB-TI.

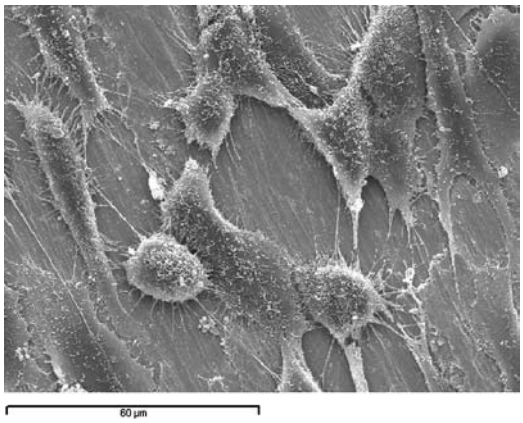

(a)

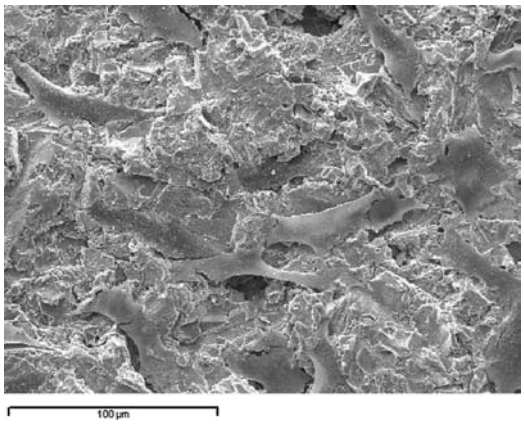

(b)

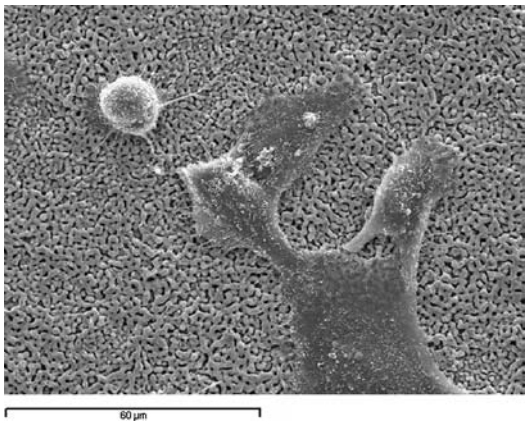

(c)

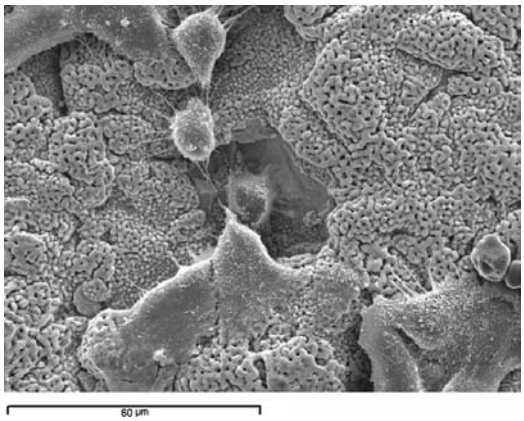

(d)

Figure 5 SEM micrograph of MG63 cells cultured for 24 hours on (a) SM-TI: machined Ti; (b): SB-TI: sandblasted Ti; (c): SM-BSP: BioSpark^{TM} treatment on SM-TI; (d) SB-BSP: BioSpark^{TM} treatment on SB-TI.

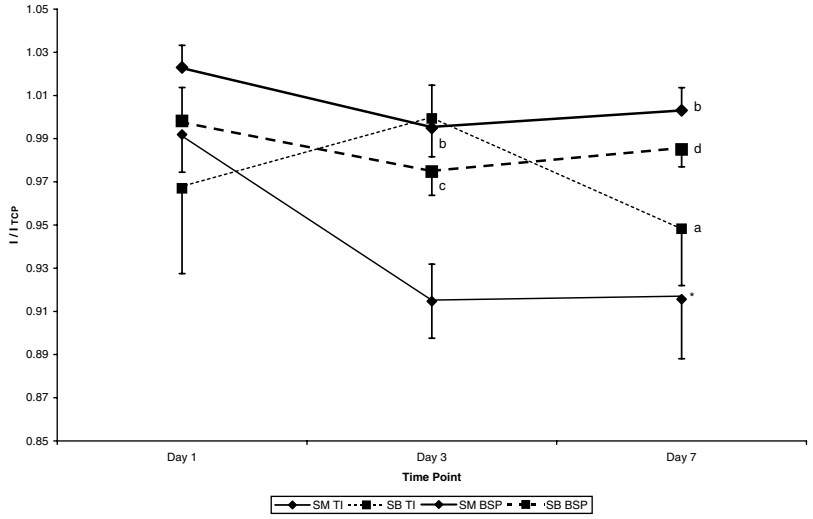

Figure 6 Results of Alamar Blue test for cell proliferation at the day 1st, 3rd and 7th of cell culturing, normalised on TCP control results. Mean ± SE, $n = 6$ triplicates. SM-TI: machined Ti; SB-TI: sandblasted Ti; SM-BSP: BioSpark^{TM} treatment on SM-TI; SB-BSP: BioSpark^{TM} treatment on SB-TI. Bonferroni multiple comparison test between tested surfaces for each experimental time: *, SM-TI *versus* SM-BSP and SB-BSP at day 7 ($p < 0.05$). Bonferroni multiple comparison test between experimental times for each tested surface: SB-TI: [a], 7 days *versus* 1 and 3 days ($p < 0.0005$); SM-BSP: [b], 1 day *versus* 3 and 7 days ($p < 0.0005$); SB-BSP: [c], 3 days ($p < 0.005$) and [d], 7 days ($p < 0.005$) *versus* 1 day.

treated samples, confirmed the 6-h post seeding findings (Fig. 4(c) and 4(d)), showing more tightly adhering cells with extended semi-transparent areas delimited by evanescent edges (Fig. 5(c) and (d)). For SB-Ti and SB-BSP (Fig. 5(b) and (d)), cells covering surface valleys were still visible but with a more flattened morphology in comparison to results at 6 h (Fig. 4(b) and (d)).

3.2.2. Cell proliferation assay

Cell proliferation results were normalised with respect to TCP control values obtained at each time point and reported in Fig. 6. All the values collected resulted quite similar to TCP results and ranged from 0.950 to 1.050.

At 1 day after cell seeding, none of the samples showed significant differences in the tested surfaces: the highest cell proliferation was observed for SM-BSP texture and the lowest for SB-TI. At 3 days, MG63 cell proliferation decreased for all the surfaces except for SB-TI, which significantly increased ($p < 0.05$) from day 1 and had the highest value, whereas SM-TI had the lowest value. Finally, at day 7, SM-TI had the lowest value ($p < 0.05$), comparable with the previous time point and cell proliferation on SB-TI, which resulted in a significant decrease ($p < 0.05$). The BSP-treated materials had the highest value, in particular for the SM-BSP surface, which had the highest value.

4. Discussion

The aim of the present study was to explore the early cell response to smooth and sandblasted Ti textures before and after surface treatment with a new, purposed bioactive method called BioSpark^{TM}. Furthermore, physicochemical characterisations were performed to know better the effect of different surface features on osteoblastic-like cellular response. The present *in vitro* findings showed a suitable cellular response with adhesion, spreading and proliferation level comparable for all the tested specimens. In particular, cell adhesion was supported by both bioactive tested materials (SM-BSP and SB-BSP) where cells anchored to the obtained nanostructured and microporous surface texture demonstrated the typical viable healthy osteoblasts traits [10]. Also proliferation assay showed that all the tested surfaces, despite their chemical and morphological differences, successfully supported osteoblasts colonisation.

In particular on day 7 of proliferation activity it showed higher values for cells cultured on both the BSP-treated surfaces than on SM-TI Ti, suggesting an enhancement in the proliferation rate, as a direct result of the surface properties of the bioactive treated Ti. The findings confirmed the results obtained in a previous study [6] for SM-BSP samples but indicate also that the biological performance of SB-TI can be markedly improved if compared to SM-TI, thanks to surface features obtained by the BioSpark^{TM} treatment.

The differences in proliferation were not significant for cells cultured on SM and SB-BSP Ti, indicating that the BioSpark^{TM} treatment induces physicochemical alterations in surface features that affect similarly cellular response, in spite of the different macroscale morphology of the treated substrates.

A decrease in cell proliferation was observed for all the materials on day 3, followed by an increase on day 7 with the exception of SB-TI. It is known from literature that osteoblastic cells show a drop in proliferation when the differentiation stage starts [6, 11].

No osteoblastic cell differentiation markers were analysed in the present study. However it seems reasonable to hypothesise that the drop in proliferation of the osteosarcoma cell line might reflect a modification in cell metabolism with cells advancing into differentiation. In this scenario, the peak in SB-TI proliferation

activity at day 3 might therefore suggest that the differentiation activity has started earlier, as indicated by the lower value observed for SB-TI on day 1, and as reported in the literature for micro-rough materials, known to enhance specific osteoblast activity instead of smoother substrata [12–15].

Regarding the physicochemical characterization of the obtained different surfaces, laser profilometry and SEM showed that SB-TI had the highest roughness value, exhibiting large valleys and high smooth plateaux. However, at high magnification, the SB-TI surface resulted smooth and did not exhibit mechanical attaching profiles for cells, which, as demonstrated preferentially, adhere to surface valley edges. Laser profilometry and SEM results were in accordance even for the other materials. SM-TI was the smoothest material with a thinner and sharper structure, and also, in agreement with the literature, the best substrata for cellular proliferation [12–15]. However, the present study showed that BioSpark^{TM} treatment induced surface modifications that enhance cellular proliferation activity, thus improving markedly the performance observed for SM-TI surface features.

EDS and TF-XRD analysis confirmed the presence of pure Ti on SM-TI surface, without contaminants due to packaging and processing. A large amount of alumina was observed on the SB surface, whose presence is viewed with great concern as a possible causative agent in impairing bone formation around pure Ti and Ti-alloy implants [16–18]. The presence of Al_2O_3 particles due to the sandblasting process was detected also on the SB-BSP sample, thus indicating that BioSpark^{TM} treatment was not effective in removing embedded Al_2O_3 particles but also that this anodic treatment did not modify Al_2O_3 particle properties, which showed high inertness to such an electrochemical treatment. Different and contrasting results were achieved by *in vitro* and *in vivo* studies on the effect of remnant Al_2O_3 blasting particles on treated surfaces. Various authors observed that Al ions dissolved by remnant blasting particles inhibited bone deposition and mineralization, the normal differentiation of bone marrow stromal cells, and the formation of calcium phosphate crystals [16, 17, 19, 20]. On the contrary, other authors reported the stimulation of bone formation both *in vitro* and *in vivo* [18, 21, 22].

In the present study *in vitro* cellular response analysis suggested that the presence of remnant Al_2O_3 blasting particles on SB-TI and SB-BSP-treated surfaces did not affect markedly cellular response as indicated by the higher proliferation activity observed on this samples on day 7 when compared to the SM-TI material. SM-BSP and SB-BSP exhibited similar surface characteristics of SM-BSP, with the exception of a spoiling presence of Al_2O_3 particles on SB-BSP.

A TiO_2 enriched by Ca and P mainly composed the SM-BSP and SB-BSP surface, which exhibited a mainly anatase structure. Recently, the stable and small crystalline anatase form of the TiO_2 has been considered for future clinical application, even though the rutile crystalline form is the most common and characterized [23, 24]. In particular, anatase plays an important role in the *in vitro* hydroxyapatite (HA) nucleation, which is also in relationship with the high *in vivo* osteointegration performance [10, 25, 26]. It is possible to hypothesise that the presence of anatase may contribute to enhancing cellular proliferation activity on BSP treated materials. Furthermore, this mainly anatase composed film is doped with calcium and phosphorus, whose role in acting as an *n*-type dopant, may be taken into account as a reasonable hypotheses. A doped oxide like this may show an increase in anatase catalytic properties, which are the main reasons for anatase capability in stimulating mineralisation processes. Indeed, it was previously demonstrated and published [7] that high Ca/P ratio showed by SM-BSP and SB-BSP typical of newly deposited bone may simulate an environment similar to that of a bony tissue in its phase of repair requiring a relatively high cell metabolic activity, thus stimulating *in vitro* cell response.

In conclusion, cellular response to BSP-treated materials may be due to the synergy of mineralising capability of anatase doped oxide and cell stimulating action of high Ca/P ratio exhibited by BSP-treated surfaces as previously reported [7]. Furthermore, even if cell response to SB-BSP might be considered slightly worse than cell response to SM-BSP, which may be justified by the presence of cells that do not stimulate inert alumina particles embedded on Ti surface due to the sandblasting process, the sandblasting operation might not be completely considered as a failure, because it promotes a highly rough texture, whose role in implant-bone mechanical stability is well known.

The present study has shown that the BioSpark^{TM} treatment performed on various surface textures enhances cellular response, and, as a consequence, potentially improves the osteointegration properties of machined and sandblasted Ti implants. This phenomenon might be due to the sub micrometric-roughness of BPS-treated samples, but also the Ca-and *P*-chemical enrichment and the crystallinity of the thick TiO_2 surface layer, mainly composed of anatase. In order to assess fully the osteointegrative properties of the developed bioactive treatment, an *in vivo* study with a suitable animal model will provide fundamental information to promote biomedical application of BioSpark^{TM} surface treatment.

Acknowledgments

The Authors wish to thank the staff of SAMM—Politecnico di Milano- Italy for their technical support, and Nanosurfaces s.r.l., a S.A.M.O. Group Company, via Matteotti 37, 40057 Cadriano di Granarolo Emilia (BO)—Italy, for providing the BioSpark^{TM}-treated materials.

References

1. R. CHIESA, E. SANDRINI, G. RONDELLI, M.SANTIN and A. CIGADA, *Journal of Applied Biomaterials & Biomechanics* **1** (2003) 91.
2. P. KURZE, W. KRYSSMAN, K.-H. DITTRICH and H.-G. SCHNEIDER, *Crystal Research and Technology* **19** (1984) 973.

3. *Idem.*, *ibid.* **19** (1984) 93.
4. E. SANDRINI, R. CHIESA, G. RONDELLI, M. SANTIN and A. CIGADA, Bachelor Thesis Politecnico di Milano T.D.L. 10116 (2002) 0TN900006823.
5. Osteointegrative interface for implantable prosthesis, a method for treating the afore mentioned interface. Patent Code: CH.02.007, Owner: POLITECNICO DI MILANO Inventors: E. Sandrini, R. Chiesa, G. Rondelli, M. Santin and A. Cigada.
6. E. SANDRINI, R. CHIESA, G. RONDELLI, M. SANTIN and A. CIGADA, *Journal of Applied Biomaterials & Biomechanics* **1** (2003) 33.
7. E. SANDRINI, C. MORRIS , R. CHIESA, A. CIGADA and M. SANTIN, *J. Biomed. Mater. Res.* **73B** (2005) 392.
8. J. LINCKS, B. D. BOYAN, C. R. BLANCHARD, C. H. LOHMANN, Y. LIU, D. L. COCHRAN, D. D. DEAN and Z. SCHWARTZ, *Biomaterials* **19** (1998) 2219.
9. C. GIORDANO, E. SANDRINI, B. DEL CURTO, E. SIGNORELLI, G. RONDELLI and L. DI SILVIO, *Journal of Applied Biomaterials & Biomechanics* **2** (2004) 35.
10. X. X. WANG , S. HAYAKAWA, K. TSURU and A. OSAKA, *J. Biomed. Mater. Res.* **52** (2000) 171.
11. L. DI SILVIO and N. GURAV, in "Human Cell Culture," edited by M. R. Koller, B. O. Palsson and J. R. W. Masters (Kluwer Academic Publishers, 2001) Vol. 5, p. 221.
12. B. D. BOYAN, T. W. HUMMERT, K. KIESWETTER, D. M. SCHRAUB, D. D. DEAN and Z. SCHWARTZ, *Scan. Electron. Microsc.* **5** (1995) 323.
13. J. E. DAVIES, B. LOWENBERG and A. SHIGA, *J. Biomed. Mater. Res.* **24** (1990) 1289.
14. D. L. COCHRAN, J.SIMPSON, H. WEBER and D. BUSER, *Int. J. Oral Maxillofac. Implants* **9** (1995) 289.
15. J. Y. MARTIN, Z. SCHWARTZ, T. W. HUMMERT, D. M. SCHRAUB, J. SIMPSON, J. LANKFORD, D. D. DEAN, D. L. CHOCRAN and R. D. BOYAN, *J. Biomed. Mater. Res.* **29** (1995) 389.
16. M. ESPOSITO, J. M. HIRSCH, U. LEKHOLM and P. THOMSEN, *Eur. J. Oral. Sci.* **106** (1998) 721.
17. W. DARWELL, N. SAMMAN, W. K. LUK, R. K. F. CLARK and H. TIDEMAN, *J. Dent.* **23** (1995) 319.
18. A. PIATTELLI, M. DEGIDI, M. PAOLANTONIO, C. MANGANO and A. SCARANO, *Biomaterials* **24** (2003) 4081.
19. G. J. THOMSON and D. A. PULEO, *ibid.* **17** (1996) 1949.
20. A. WENNERBERG, T. ALBREKTSSON, C. JOHANSSON and B. ANDERSSON, *ibid.* **17** (1996) 15.
21. J. E. FEIGHAN, V. M. GOLDBERG, D. DAVY, J. A. PARR and S. STEVENSON, *J. Bone Joint Surg.* **77A** (1995) 1380.
22. K. H. LAU, A. YOO and S. P.WANG, *Mol. Cell. Biochem.* **105** (1991) 93.
23. F. H. JONES, *Surface Science Reports* **42** (2001) 75.
24. G. GIAVARESI, L. AMBROSIO, G. A. BATTISTON, U. CASELLATO, R. GERBASI, M. FINI, N. N. ALDINI, L. MARTINI, L. RIMONDINI and R. GIARDINO, *Biomaterials* **25** (2004) 5583.
25. M. UCHIDA, H. KIM, X. ZHANG and T. KOKUBO, *ibid.* **25** (2004) 1003.
26. S. KANEKO, K. TSURU, S. HAYAKAWA, S. TAKEMOTO, C. OHTSUKI, T. OZAKI, H. INOUE and A. OSAKA, *ibid.* **22** (2001) 875.

Received 30 June
and accepted 18 July 2005